Supporting Information for:

Pre-Assembled Fluorescent Multivalent Probes for Imaging of Anionic Membranes

Felicia M. Roland, Evan M. Peck, Douglas R. Rice, and Bradley D. Smith*

Department of Chemistry and Biochemistry, 236 Nieuwland Science Hall, University of Notre Dame, Notre Dame, Indiana 46556, USA

*E-mail: smith.115@nd.edu

Contents

A. Probe Synthesis and Structural Characterization

Materials and Equipment

Commercially available solvents and chemicals were purchased from Sigma-Aldrich, Alfa-Aesar, and VWR International and used without further purification unless otherwise stated. Water was de-ionized and microfiltered. Reactions were monitored by TLC plate (precoated with 60 Å silica gel, F-254) purchased from SiliCycle and visualized either by UV light (254, 365 nm) or iodine stain. Flash column chromatography was performed using silica gel (silicaFlash P60 from SiliCycle) as the stationary phase. NMR spectra were recorded on Bruker AVANCE III HD 400, 500 MHz or Varian INOVA-600 MHz spectrometer. Chemical shift is presented in ppm and referenced by residual solvent peak. Mass spectrometry (MS) was performed using a Bruker microTOF II or a Bruker AutoflexIII smartbeam spectrometer.

Probe Synthesis

The untargeted pre-assembled probes **6C** ⊃ **S** and **2(6C)** ⊃ **S3S** were prepared as reported previously.[S1]

Synthesis of Macrocycle **6Z**

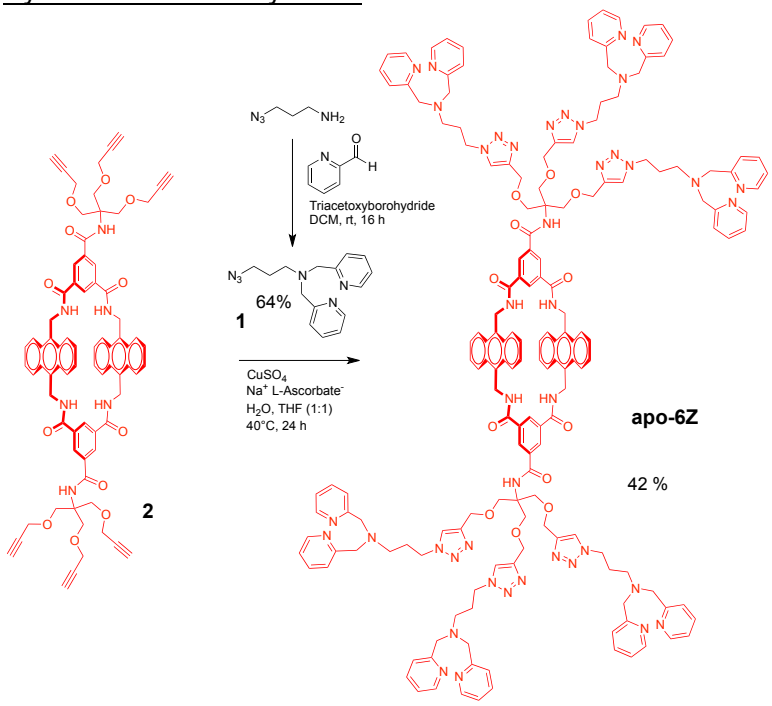

Azidopropylamine (1g, 10 mmol), pyridine-2-carboxaldehyde (3.8 mL, 4 eq), and triacetoxyborohydride (6.4 g, 3 eq) were placed in a dry round bottomed flask containing 100 mL of anhydrous dichloromethane and activated molecular sieves (3 μm). The reaction was stirred at room temperature under argon for 16 hours, after which time the reaction was diluted with dichloromethane (100 mL). The organic layer was washed with saturated $NaHCO_3$ (2 x 100 mL) and dried over Na_2SO_4, filtered, and the solvent removed under reduced pressure. The remaining residue was purified by silica gel column chromatography using 0-5% methanol in chloroform as eluent to yield the pure product **1** as a brown, viscous oil (1.8 g, 64%) ^{1}H NMR (500 MHz, $CDCl_3$, 25 °C): δ 8.54 (ddd, *J* = 4.8, *J* = 1.7, *J* = 0.9 Hz, 2H), 7.67 (td, *J* = 7.6, *J* = 1.8 Hz, 2H), 7.51 (d, *J* = 7.6 Hz, 2H), 7.14 - 7.20 (m, 2H), 3.84 (s, 4H), 3.31 (t, *J* = 6.9 Hz, 2H), 2.66

(t, *J* = 6.9 Hz, 2H), 1.81 (quin, *J* = 6.8 Hz, 2H). ^{13}C NMR (150 MHz, $CDCl_3$, 25 °C): δ 159.2, 148.8, 136.2, 122.7, 121.8, 60.3, 51.0, 49.2, 26.4 HRMS (ESI-TOF): calculated for $C_{15}H_{19}N_6$ $[M+H]^+$ 283.1666, found 283.1639.

Hexa-alkyne macrocycle **2**[S1] (40 mg, 32 µmol) and azide **1** (72 mg, 250 µmol) were dissolved in tetrahydrofuran (4 mL) that had been purged with argon (5 min) in a small vial. In a separate vial, copper (II) sulfate (82 mg, 10 eq) and sodium L-ascorbate (64 mg, 10 eq) were dissolved in H_2O also purged with argon. The solutions were combined and the mixture was stirred at 50 °C for 6 hours. At this time, saturated EDTA solution (20 mL) and brine (50 mL) was added, and the mixture was extracted with chloroform (5 x 50 mL), dried over Na_2SO_4, filtered and the solvent removed under reduced pressure. The residue was purified by silica gel column chromatography in 100% acetone to removed starting **4**, then 0-20% methanol in chloroform to remove excess **1**, followed by 80:19:1 $CHCl_3$:MeOH:NH_4OH to elute the product. The brown, sticky solid was washed with cold acetonitrile (5 mL), then cold acetone (5 mL) to yield pure **apo-6Z** as a light brown, flaky solid (40 mg, 42%). ^{1}H NMR (600 MHz, DMSO-d_6, 25 °C): δ 8.79 (br. s., 4H), 8.42 (d, *J* = 4.4 Hz, 12H), 8.40 (s, 4H), 8.29 - 8.35 (m, 8H), 8.03 (s, 2H), 7.97 (s, 6H), 7.69 (t, *J* = 7.6 Hz, 12H), 7.45 (d, *J* = 7.8 Hz, 12H), 7.41 (s., 8H), 7.15 - 7.23 (m, 12H), 5.38 (s, 8H), 4.51 (s, 12H), 4.36 (t, *J* = 7.1 Hz, 12H), 3.82 (s, 12H), 3.71 (s, 24H), 2.47 (t, *J* = 6.8 Hz, 12H), 2.07 (quin, *J*=6.7 Hz, 12 H). ^{13}C NMR (150 MHz, DMSO-d_6, 25 °C): δ 165.9, 165.8, 159.0, 148.7, 143.9, 136.4, 135.7, 134.3, 130.3, 129.9, 129.7, 125.6, 125.1, 123.6, 122.7, 122.1, 79.2, 67.6, 64.2, 60.6, 59.5, 50.3, 47.5, 36.0, 27.4. HRMS (ESI-TOF): calculated for $C_{166}H_{175}N_{42}O_{12}$ $[M+H]^+$ 2948.4369, found 2948.4380. **Apo-6Z** (43 mg, 0.14 µmol) and $Zn(NO_3)_2.6H_2O$ (25 mg, 90 µmol) were dissolved in a mixture of methanol (2.0 mL) and water (0.2 mL). The mixture was stirred at room temperature for half an hour, then evaporated under vacuum to provide the zinc complex, **6Z**, which was dissolved in deionized water (1.0 mL) to give a stock solution.

Pre-assembly of Threaded Fluorescent Probes

Separate stock solutions (1.0 mM) were prepared of **S**, **6Z** and **6C** in water, and **S3S** in 1:3 DMSO:H_2O. Aliquots were combined in the appropriate stoichiometry, producing a final concentration for added squaraine scaffold (**S** or **S3S**) of 250 µM. After waiting to ensure complete threading (few minutes in the case of **6C** ⊃ **S** and **6Z** ⊃ **S**, few hours in the case of **2(6C)** ⊃ **S3S** and **2(6Z)** ⊃ **S3S**), the photophysical properties were determined after diluting an aliquot of each pre-assembled probe to 3.0 µM. The measured values of molar absorptivity and fluorescence quantum yield are listed in manuscript Table 1. Molar absorptivities were determined at concentrations of 1.0 µM, 3.0 µM, and 5.0 µM and the values were averaged. An absorbance of 0.08 (3.0 µM of probe) was used to measure the quantum yield relative to methylene blue (Φ_f = 0.02 in H_2O).[S2] All measurements were made in triplicate.

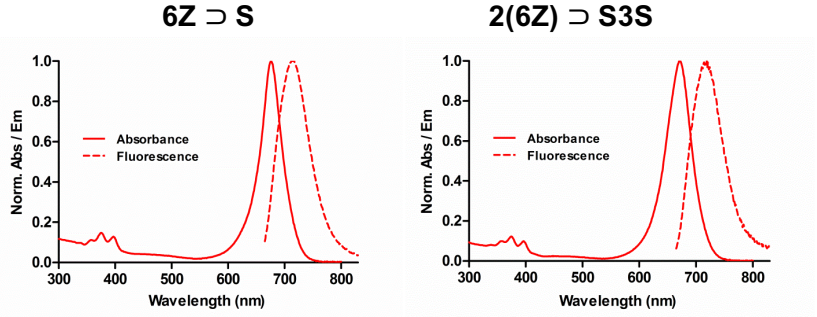

Figure S1. Absorption and emission spectra (Ex: 650 nm) in water for pre-assembled probes **6Z** ⊃ **S** and **2(6Z)** ⊃ **S3S**.

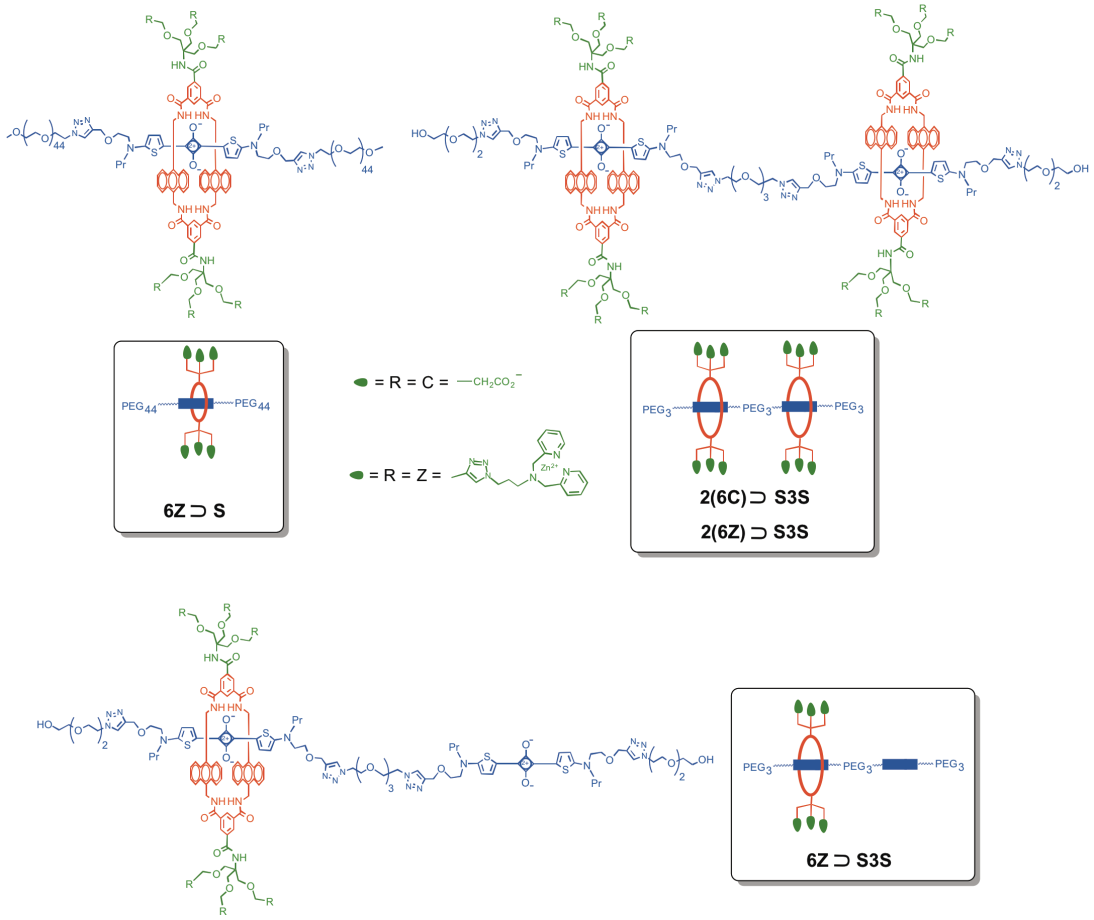

Scheme S1. Structures of singly and doubly threaded fluorescent probes.

Structural Proof and Spectral Properties of Threaded Fluorescent Probes

The threaded structures of **6C** ⊃ **S** and **2(6C)** ⊃ **S3S** were characterized by a combination of ^{1}H NMR, UV/Vis, fluorescence spectroscopy, mass spectrometry, and gel electrophoresis as previously reported.[S1] The threaded structures of new probes **6Z** ⊃ **S** and **2(6Z)** ⊃ **S3S** were indicated by diagnostic changes in squaraine optical properties, including a characteristic 20-30 nm red-shift in absorption and fluorescence maxima, and efficient internal energy transfer from the anthracene side-walls in the surrounding macrocycle (Ex: 390 nm) to the encapsulated squaraine dye (Ex: 710 nm).[S1]

Additional absorption and fluorescence titration studies were conducted to prove the doubly threaded structure of **2(6Z)** ⊃ **S3S**. As shown in Figure S2, addition of one molar equivalent of **6Z** to a solution of two-station squaraine scaffold **S3S** produced the single threaded two station complex **6Z** ⊃ **S3S** (see Scheme S1 for chemical structure) and a large (~50 nm) red-shift in absorbance (Figure S2a), coupled with an increase in fluorescence emission at ~715 nm and an increase in energy transfer emission. Subsequent addition of a second equivalent of macrocycle produced the doubly threaded two station complex **2(6Z)** ⊃ **S3S** and a further 9 nm red shift in absorbance (Figure S2a), a two-fold increase in both the fluorescence emission (Figure S2b) and internal energy transfer emission (Figure S2c).

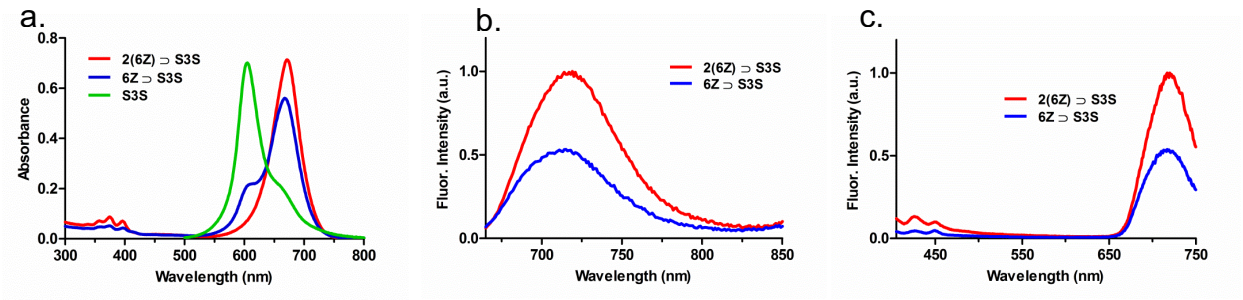

Figure S2. a) Absorbance spectra (3.0 μM, 25°C) of free two-station squaraine scaffold **S3S** (green), single threaded two station complex **6Z** ⊃ **S3S** (blue), and doubly threaded two station complex **2(6Z)** ⊃ **S3S** (red). b) Fluorescence (3.0 μM, 25°C, Ex: 650 nm) of single threaded two station complex **6Z** ⊃ **S3S** (blue), and doubly threaded two station complex **2(6Z)** ⊃ **S3S** (red). c) Internal energy transfer (3.0 μM, 25°C, Ex: 390 nm) of single threaded two station complex **6Z** ⊃ **S3S** (blue), and doubly threaded two station complex **2(6Z)** ⊃ **S3S** (red).

Shown in Figure S3 is an additional time-course study that monitored the time-dependent change in fluorescence emission intensity caused by step-wise threading of two copies of macrocycle **6Z** onto the two-station scaffold **S3S** to initially form **6Z** ⊃ **S3S** and then form **2(6Z)** ⊃ **S3S**. The step-wise threading profile is the same as that observed previously with an analogous system that sequentially threaded two copies of a structurally similar macrocycle onto the two-station scaffold **S3S**.[S1]

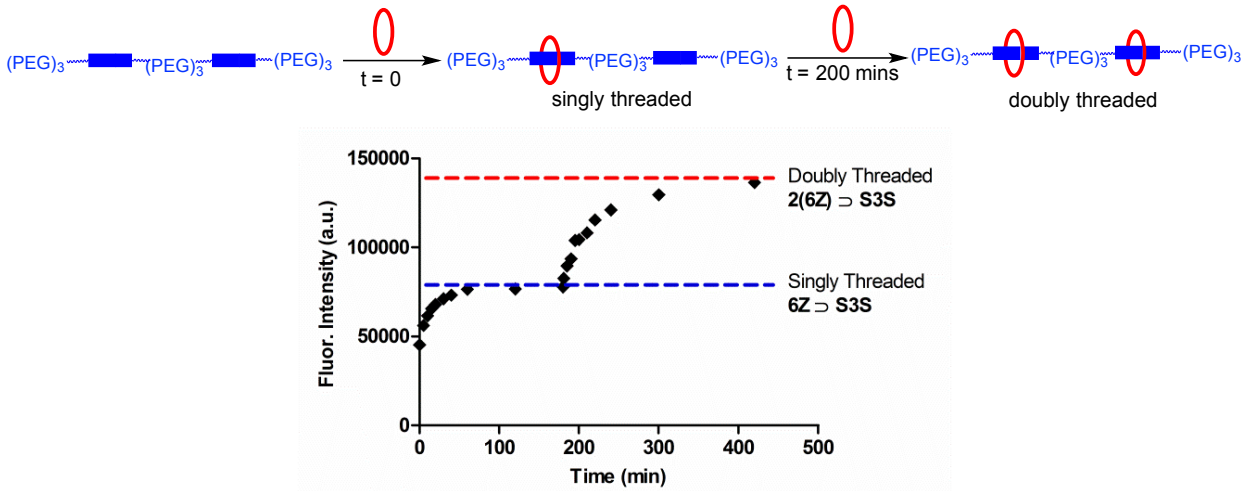

Figure S3. Time-dependent fluorescence enhancement due to step-wise threading of two copies of macrocycle **6Z** onto the two-station scaffold **S3S**. The experiments started at t = 0 by adding one molar equivalent of **6Z** to a solution of **S3S** (250 μM) to form **6Z** ⊃ **S3S**, and once threading was complete (t = 200 minutes) a second molar equivalent of the macrocycle was added to the solution to form **2(6Z)** ⊃ **S3S**. Ex 670 nm, Em = 715 nm, T = 25 °C.

Two other structural elucidation techniques, ^{1}H NMR spectroscopy and MALDI-TOF mass spectrometry, were investigated as independent methods to confirm that probe pre-assembly had occurred. Shown in Figure S4 are partial ^{1}H NMR showing the expected diagnostic changes

in chemical shift upon formation of **6Z** ⊃ **S**. Also observed are the expected minor signals corresponding to a small fraction of encapsulated squaraine in a *cis* conformation (thiophene units point to the same side).[S1] The ^{1}H NMR spectrum for **2(6Z)** ⊃ **S3S** was very broad and featureless, consistent with spectra of related two-station threaded complexes and suggestive of dynamic processes that match the NMR time-scale.[S1] MALDI-TOF mass spectrometry was performed using a Bruker AutoflexIII smartbeam equipped with an all-solid-state laser (355 nm wavelength). Aliquots of pre-assembled complex (**6Z** ⊃ **S** or **2(6Z)** ⊃ **S3S**) and 0.7 μL of a saturated 2,5-dihydroxybenzoic acid solution (matrix) were combined on the MALDI sampling plate, allowed to dry for 30 minutes, then a MALDI-TOF mass spectrum was obtained using, linear detection, Grating/Cut-off: Up to 1000 MW, Ion Source 1: 20.05 V, Ion Source 2: 18.45 V, lens: 7.31 V. With each separate sample there was clear evidence for the presence of the threaded structure with correct stoichiometry (Figure S5).

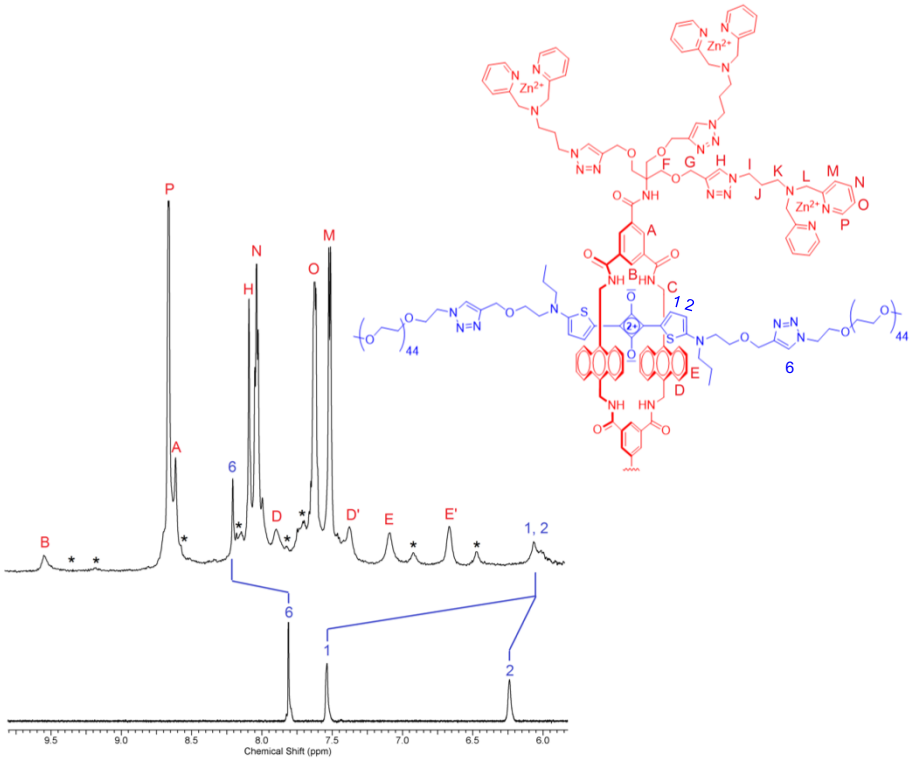

Figure S4. Partial ^{1}H NMR (600 MHz, D_2O, 25 °C) of: (top) **6Z** ⊃ **S** (2.0 mM); (bottom) squaraine scaffold **S** (2.0 mM). Blue lines indicate major changes in chemical shift upon complexation. *Denotes signals from minor squaraine *cis* conformational isomer. Note: The ^{1}H NMR spectrum of free macrocycle **6Z** was very broad and so it was not included.

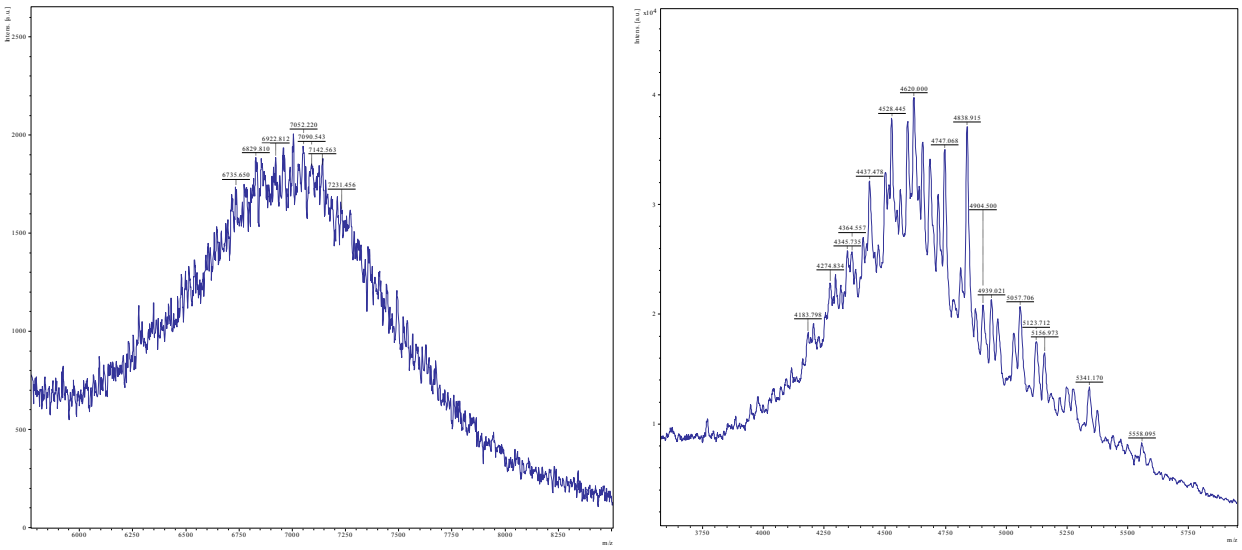

Figure S5. MALDI-TOF spectra showing molecular ion peaks for **6Z** ⊃ **S** (*left*) and **2(6Z)** ⊃ **S3S** (right). In each case the peaks are broad due to the polydisperse PEG chain molecular weight and/or polydisperse number of associated Zn^{2+} and NO_3^- counter ions within the strongly acidic matrix.

B. Liposome Studies

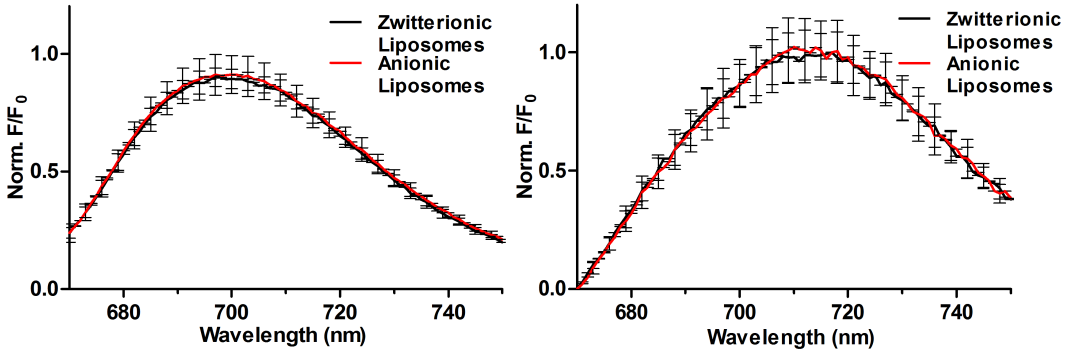

Figure S6. Fluorescence spectra showing no fluorescence turn-on for control probes: (*left*) **6C** ⊃ **S**, (*right*) **2(6C)** ⊃ **S3S** (250 nM) in the presence of either of either zwitterionic (100% POPC) or anionic (20% POPS, 80% POPC) liposomes (total phospholipid 1 mM), Ex: 645 nm.

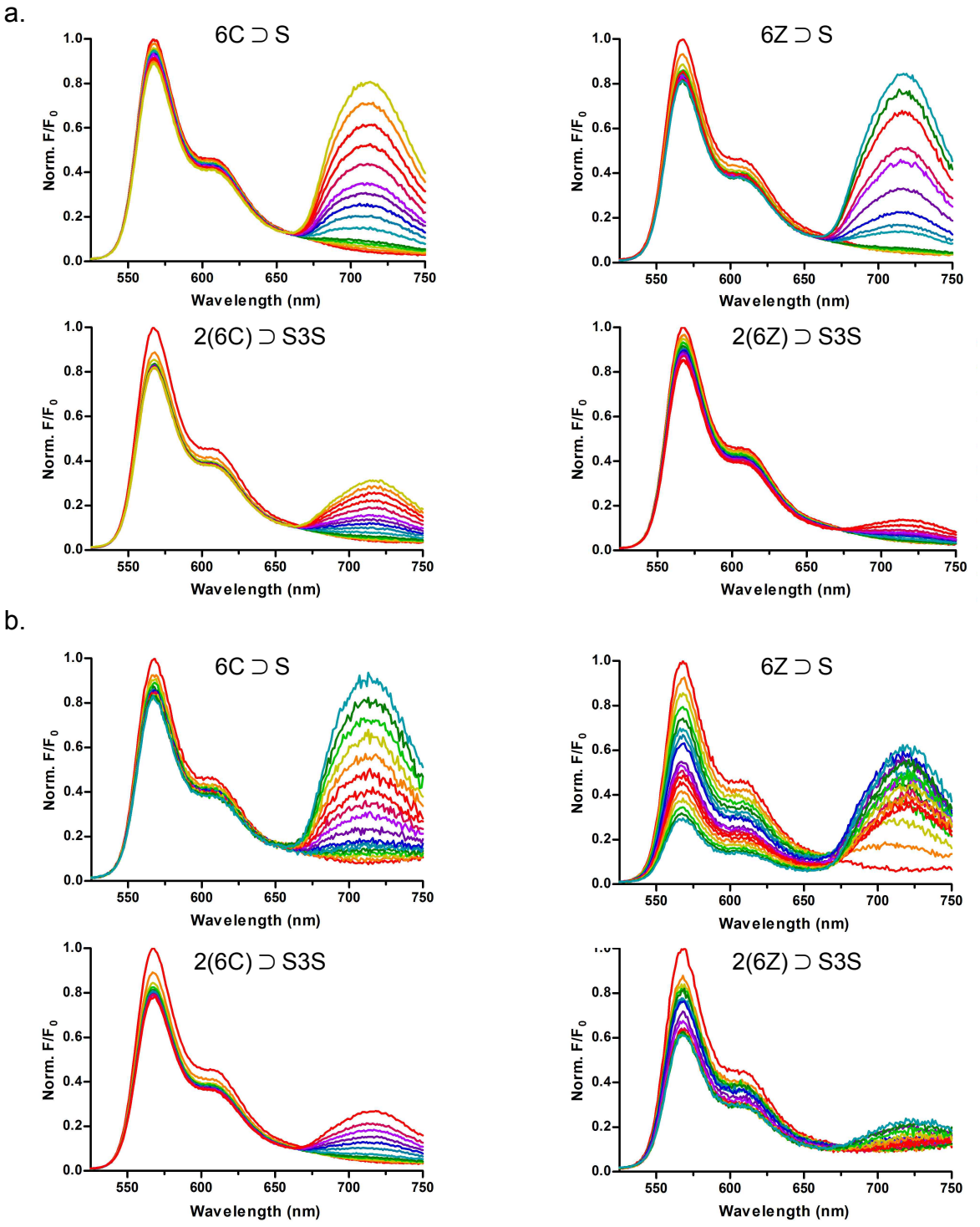

Figure S7. Representative set of FRET titration spectra for: a) zwitterionic liposomes (99% POPC, 1% $DiIC_{18}$) and b) anionic liposomes (20% POPS, 79% POPC, 1% $DiIC_{18}$) (total lipid concentration 2 μM). Probe concentrations during the titration ranged from 0-800 nM, Ex: 480 nm.

It is worth noting some subtle differences between the FRET titration spectra in Figure S7. The two control probes **6C** ⊃ **S** and **2(6C)** ⊃ **S3S** are weakly fluorescent at 720 nm when excited at 480 nm. Since they do not associate with anionic or zwitterionic liposomes, they do not quench $DiIC_{18}$ by FRET and their 720 emission bands only show weak incremental increase in intensity as the titration progresses. The two targeted probes **6Z** ⊃ **S** and **2(6Z)** ⊃ **S3S** are also weakly fluorescent at 720 nm when excited at 480 nm. When they associate with anionic liposomes there is substantial $DiIC_{18}$ quenching by FRET. But as shown in manuscript Figure 8 there is a non-linear change in the 720 emission bands due to probe self-aggregation and self-quenching on the liposome surface.

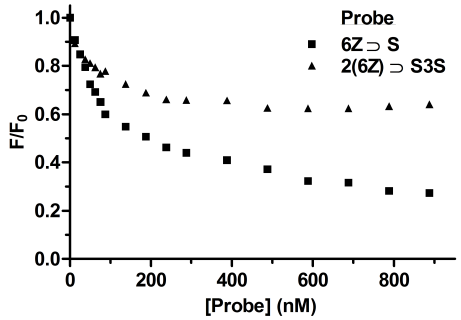

Figure S8. Overlay of titration isotherms for quenching of $DiIC_{18}$ fluorescence at 568 nm due to FRET caused by association of probes **6Z** ⊃ **S** and **2(6Z)** ⊃ **S3S** with anionic liposomes.

Inspection of Figure S8 shows that the titration isotherm for **2(6Z)** ⊃ **S3S** reaches saturation well before the titration isotherm of **6Z** ⊃ **S**, indicating that the dodecavalent probe has higher membrane affinity than the hexavalent probe. However, the extent of $DiIC_{18}$ quenching by hexavalent **6Z** ⊃ **S** is greater, indicating that energy transfer from the membrane-bound $DiIC_{18}$ to membrane-bound **6Z** ⊃ **S** is more efficient than membrane-bound **2(6Z)** ⊃ **S3S**. The fluorophores are the same in each case; thus, the average distance from membrane-bound $DiIC_{18}$ to membrane-bound **6Z** ⊃ **S** must be shorter than the average distance to membrane-bound **2(6Z)** ⊃ **S3S**. This is expected since the dodecavalent **2(6Z)** ⊃ **S3S** has a higher cationic charge and repels the cationic $DiIC_{18}$ more than the hexavalent **6Z** ⊃ **S**, thus increasing the average distance between FRET partners and decreasing the FRET efficiency.

C. Additional Cell Microcopy Images

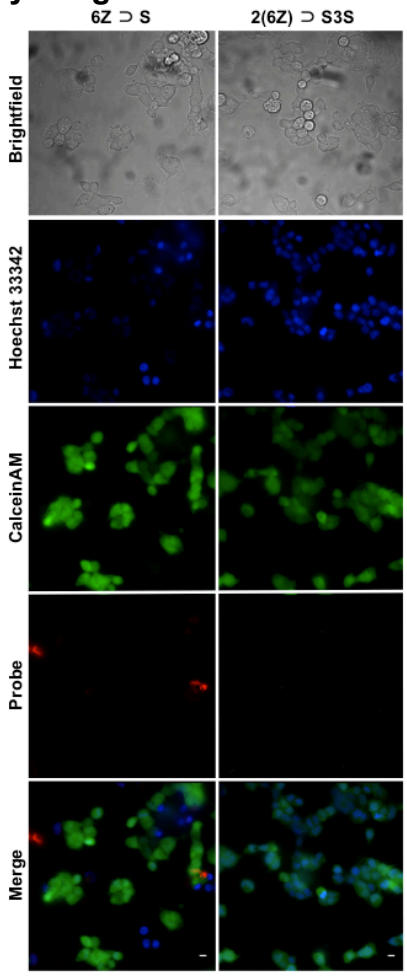

Figure S9. Fluorescence microscopy images of healthy PAIII cells (not treated with staurosporine) after incubation with 1 µM of deep-red **6Z** ⊃ **S** or **2(6Z)** ⊃ **S3S** and costained with blue Hoechst33342 (3 µM) and green CalceinAM (5 µM). Scale Bar = 10 µM

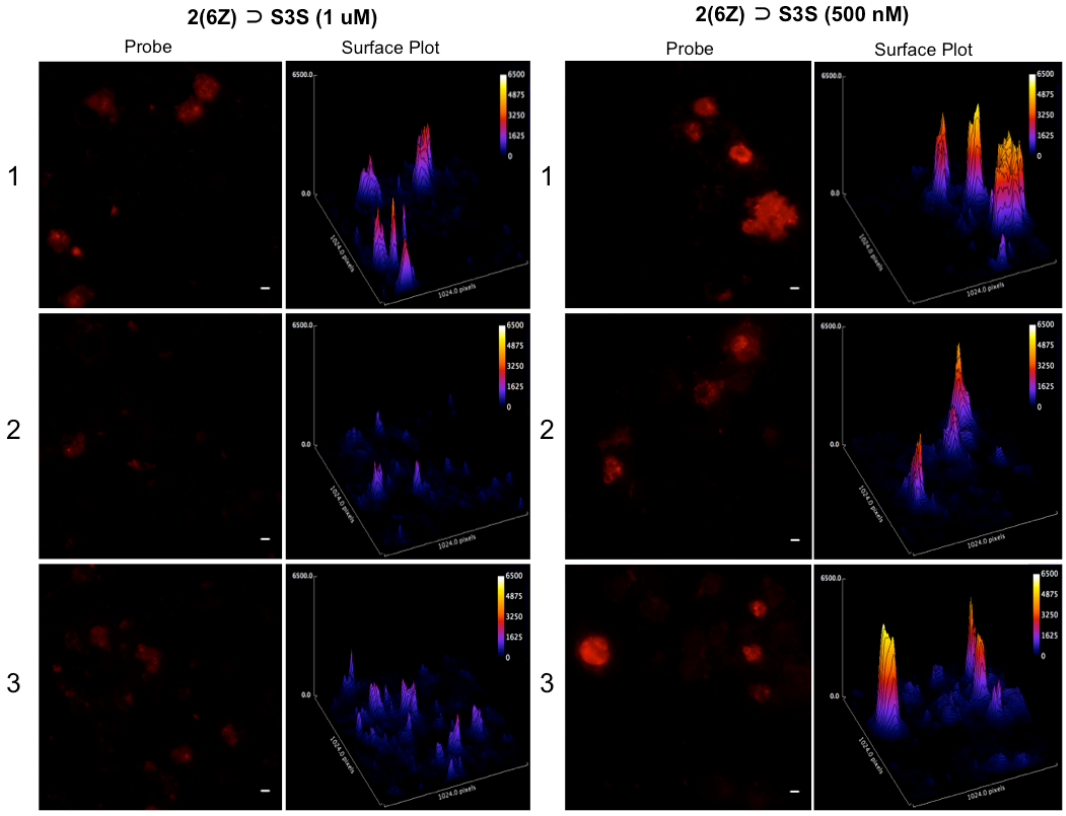

Figure S10. Three sets of fluorescence microscopy images of dead and dying PAIII cells caused by treatment with staurosporine and subsequently stained with **2(6Z) ⊃ S3S**. The surface plots show that average deep-red probe fluorescence intensity for cells stained with 1 μM of **2(6Z) ⊃ S3S** (*left*) is lower than cells stained with 500 nM of **2(6Z) ⊃ S3S** (*right*) The plots were generated using ImageJ software and normalized to a scale of 0-6500 (a.u). Scale bar = 10 μM.

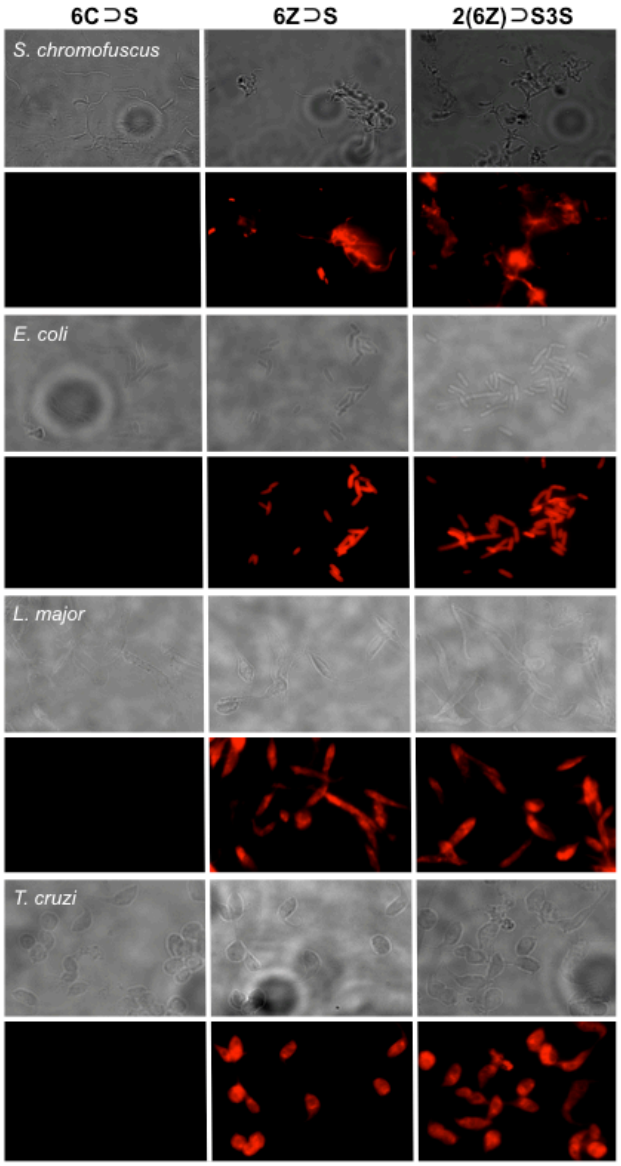

Figure S11. Fluorescence micrographs of live *S. chromofuscus*, *E. coli*, *L. major*, and *T. cruzi*, treated with **6C** ⊃ **S**, **6Z** ⊃ **S**, or **2(6Z)** ⊃ **S3S** (5.0 μM). Brightfield (upper panel) and deep-red probe fluorescence (lower panel). The fluorescence intensity of each image is scaled differently so as to reveal the microbial staining pattern.

D. ^{1}H and ^{13}C NMR Spectra

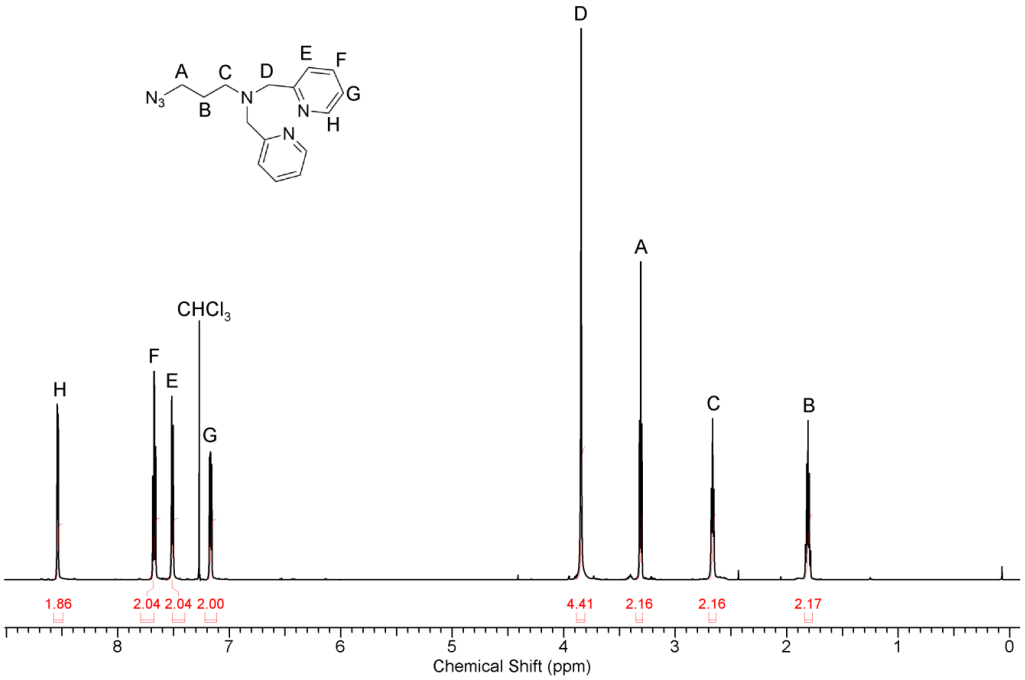

^{1}H NMR (500 MHz, $CDCl_3$, 25 °C) spectrum of **5**.

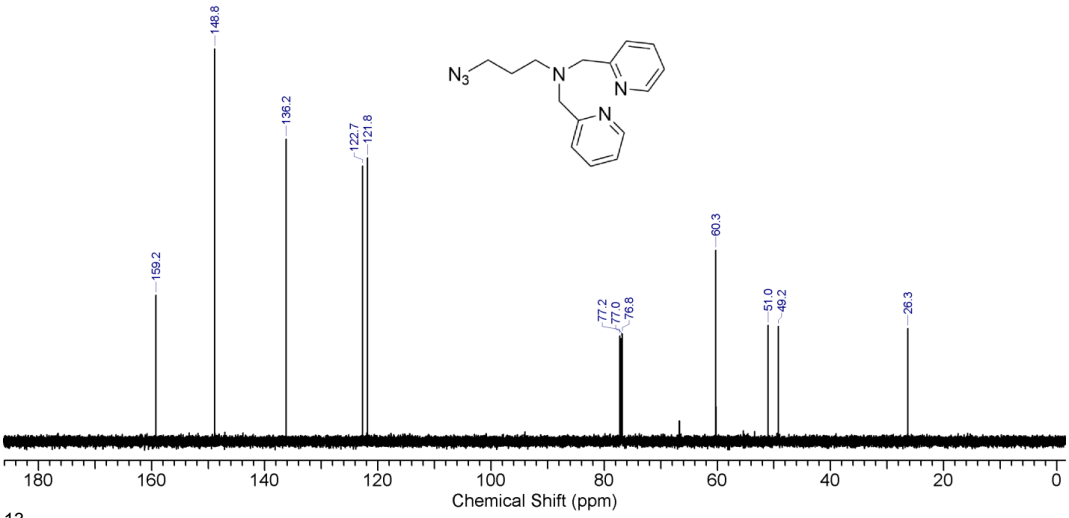

^{13}C NMR (150 MHz, $CDCl_3$, 25 °C) spectrum of **5**.

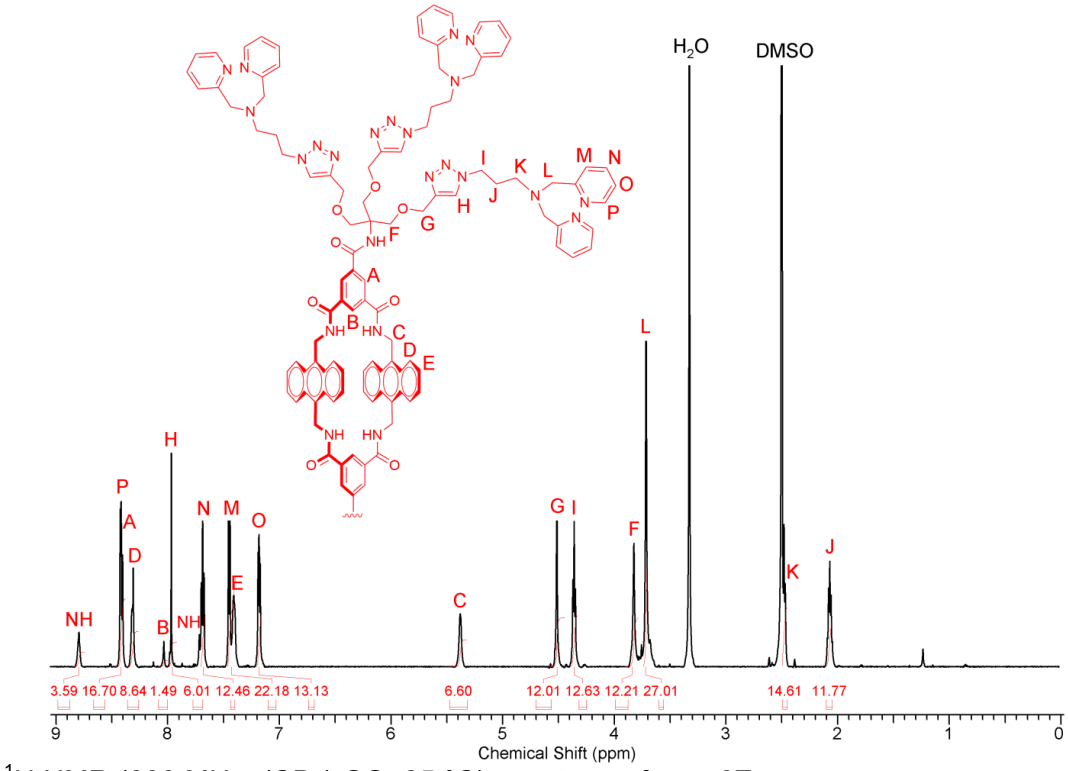

^{1}H NMR (600 MHz, $(CD_3)_2SO$, 25 °C) spectrum of **apo-6Z**.

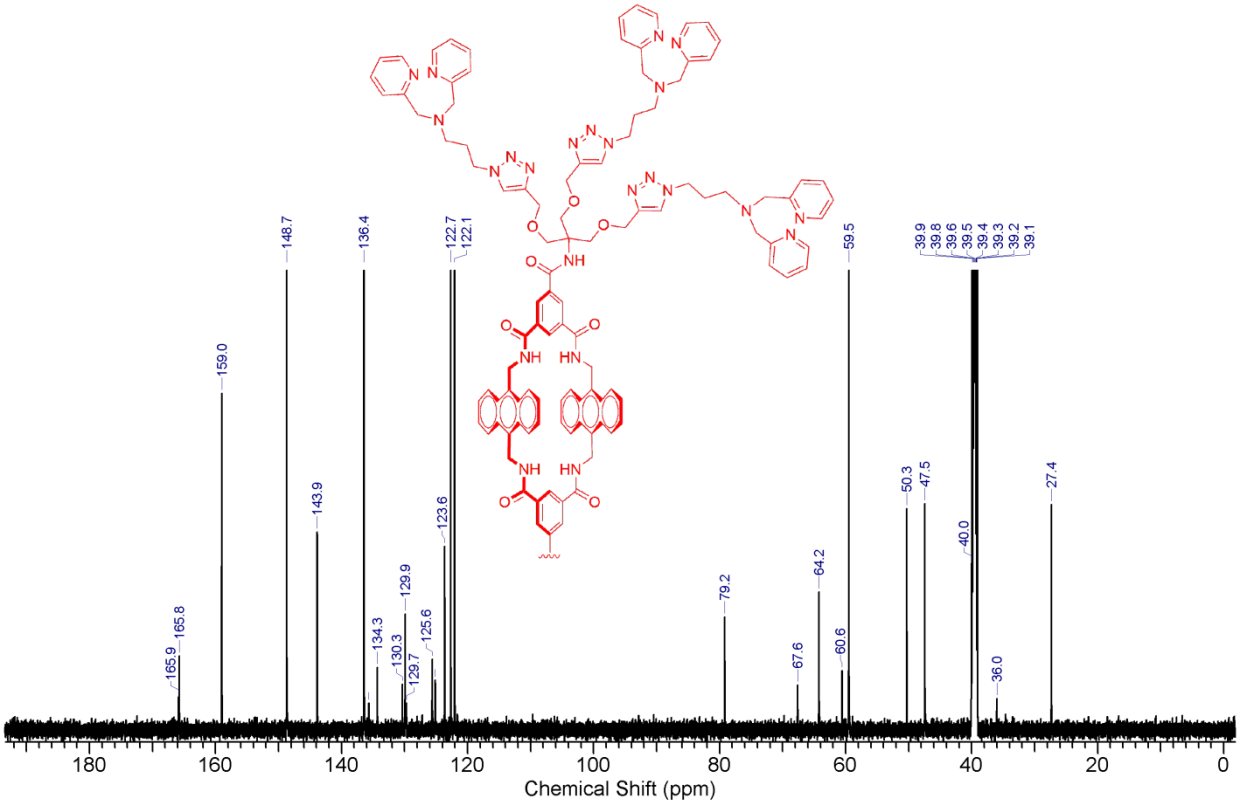

^{13}C NMR (150 MHz, $(CD_3)_2SO$, 25 °C) spectrum of **apo-6Z**.

E. References

(S1) Peck, E., Battles, P., Rice, D., and Roland, F. (2016) Pre-assembly of near-infrared fluorescent multivalent molecular probes for biological imaging. *Bioconjugate Chem. 27*, 1400–1410.
(S2) Atherton, S. J., and Harriman, A. (1993) Photochemistry of intercalated methylene blue: photoinduced hydrogen atom abstraction from guanine and adenine. *J. Am. Chem. Soc. 115*, 1816–1822.
(S4) Liu, W., Peck, E. M., Hendzel, K. D., and Smith, B. D. (2015) Sensitive structural control of a macrocycle threading by a fluorescent squaraine dye flanked by polymer chains. *Org. Lett. 17*, 5268–5271.
(S5) Ke, C., Destecroix, H., Crump, M. P., and Davis, A. P. (2012) A simple and accessible synthetic lectin for glucose recognition and sensing. *Nat. Chem. 4*, 718–723.